



## 2 Estimating fractional sky cover from spectral measurements

3 Qilong Min,<sup>1</sup> Tianhe Wang,<sup>1,2</sup> Charles N. Long,<sup>3</sup> and Minzheng Duan<sup>4</sup>

4 Received 15 April 2008; revised 14 August 2008; accepted 29 August 2008; published XX Month 2008.

5 [1] A method for estimating fractional sky cover from spectral measurements has been  
6 developed. The spectral characteristics of clouds and clear-sky aerosols are utilized to  
7 partition sky fraction. As illustrated in our sensitivity study and demonstrated in real  
8 measurements, the transmittance ratio at selected wavelengths is insensitive to solar zenith  
9 angle and major atmospheric gaseous absorption. With a localized baseline procedure,  
10 retrievals of this ratio method are independent of absolute calibration and weakly sensitive  
11 to changes in cloud and aerosol optical properties. Therefore this method substantially  
12 reduces the retrieval uncertainty. The uncertainty of this method, estimated through the  
13 sensitivity study and intercomparison, is less than 10%. With globally deployed  
14 narrowband radiometers, this simple ratio method can substantially enhance the current  
15 capability for monitoring fractional sky cover.

16 **Citation:** Min, Q., T. Wang, C. N. Long, and M. Duan (2008), Estimating fractional sky cover from spectral measurements,  
17 *J. Geophys. Res.*, 113, XXXXXX, doi:10.1029/2008JD010278.

### 19 1. Introduction

20 [2] Clouds remain the greatest sources of uncertainty in  
21 global climate change research [IPCC, 2007]. The impact of  
22 greenhouse warming on cloud amount through climate  
23 feedback will have significant changes on the global radi-  
24 ative energy balance [Randall *et al.*, 1984]. Variations of  
25 cloud cover have significantly contributed to contemporary  
26 climatic changes. Thus it is crucial to accurately monitor  
27 fractional sky cover of clouds globally.

28 [3] Monitoring cloud amount has a long history: from  
29 earlier human-empirical sky observations, to surface passive  
30 and active measurements [Fairall and Hare, 1990; Clothiaux  
31 *et al.*, 1999; Long and Ackerman, 2000; Pfister *et al.*, 2003;  
32 Long *et al.*, 2006a, 2006b], to recent satellite retrievals  
33 [Minnis, 1989; Rossow *et al.*, 1993]. Satellite observations  
34 provide the global coverage of cloud amount to study global  
35 climate change. Their limits in spatial/temporal resolution  
36 and issues with surface influences manifest the need for  
37 surface measurements to verify satellite retrievals and to fill  
38 the gaps between satellite observations. Current technology  
39 has advanced in surface observations of cloud amounts from  
40 human-empirical sky observations, to spatial estimation  
41 from sky imagers, to temporal estimation of cloud occur-  
42 rences from passive and active sensors. However, even with  
43 an increasing number of sky imagers and other passive and  
44 active sensors for monitoring cloud fraction, there are still  
45 limited surface measurements available to date.

[4] Since shortwave (SW) radiation is strongly modulated 46  
by clouds, widely deployed spectral and broadband short- 47  
wave radiometers provide the potential to estimate cloud 48  
fraction in large geographic distribution. Long *et al.* [2006a] 49  
proposed a methodology for inferring fractional sky cover 50  
from broadband SW diffuse irradiance measurements during 51  
daylight hours. Their method utilizes the enhancement of 52  
diffuse irradiance under cloudy conditions to partition 53  
cloudy and clear-sky fractions, through a normalization 54  
procedure to remove solar zenith angle dependences. Since 55  
clouds and aerosols (clear-sky) with different particle sizes 56  
exhibit significant differences of spectral dependences of 57  
optical properties, there is a possibility to estimate sky cover 58  
using spectral measurements of narrowband radiometers. 59

### 2. Spectral Ratio and Retrieval Algorithm 60

[5] The spectral dependence of optical depth of atmo- 61  
spheric scatterers generally follows Angstrom's empirical 62  
relationship [Angstrom, 1929]: 63

$$\tau_{sca}(\lambda) = \beta\lambda^{-\alpha} \quad (1)$$

where  $\tau_{sca}(\lambda)$  is the optical depth of atmospheric scatterers 65  
at wavelength  $\lambda$ ,  $\beta$  and  $\alpha$  are constants. More importantly, 66  
the Angstrom exponent  $\alpha$  is an indicator of the size of the 67  
scatterers. For molecules in the Rayleigh scattering regime, 68  
its value approaches 4, while for cloud particles in the Mie 69  
scattering regime, it is close to 0. For aerosol particles, the 70  
Angstrom exponent varies between Rayleigh and clouds, 71  
with a typical value of about 1.3. Because of such spectral 72  
dependence of optical depth, the diffuse transmittance ratio 73  
between a longer wavelength and a short wavelength is 74  
about 1 for clouds, and less than 1 for aerosols, respectively, 75  
as illustrated in Figure 1. On the basis of this physical 76  
principle and further sensitivity study below, the baselines 77  
of transmittance ratio under both aerosol and cloud 78

<sup>1</sup>Atmospheric Sciences Research Center, State University of New York, Albany, New York, USA.

<sup>2</sup>College of Atmospheric Sciences, Lanzhou University, Lanzhou, China.

<sup>3</sup>Pacific Northwest National Laboratory, Richland, Washington, USA.

<sup>4</sup>Institute of Atmospheric Physics, Chinese Academy of Science, Beijing, China.

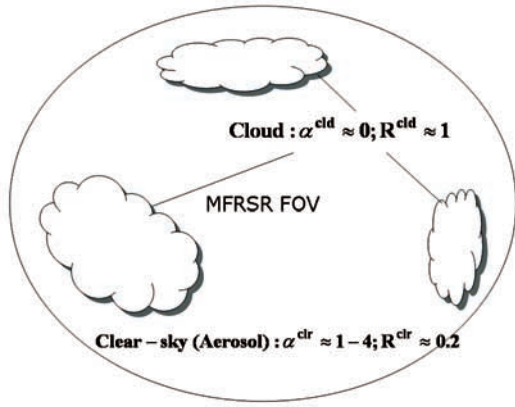


**Figure 1.** Sketch of retrieval principle of cover fractional cover.  $\alpha$  is the Angstrom exponent and  $R$  is the transmittance ratio at two wavelengths; cld and clr represent cloud and clear-sky conditions, respectively.

79 conditions are well defined and less sensitive to variations  
80 of both aerosol and cloud properties. A measured  
81 transmittance ratio in reality is weighted by the cloud  
82 amount in the sky and can be assumed as a linear partition  
83 between cloud transmittance ratio and clear-sky transmittance  
84 ratio:

$$R^{obs} = (1 - \phi)R^{clr} + \phi R^{cld} \quad (2)$$

86 where  $\phi$  is the fractional sky cover in the atmosphere.  
87 Therefore fractional sky cover can be inferred from a simple  
88 analytical expression

$$\phi = \frac{R^{obs} - R^{clr}}{R^{cld} - R^{clr}} \quad (3)$$

91 [6] As solar transmittances at different wavelengths vary  
92 with solar zenith angle systematically, the transmittance  
93 ratio at two wavelengths is less dependent on solar zenith  
94 angle (or time). If a basic set of cloudy and clear-sky  
95 transmittances is defined at any given time (or solar zenith  
96 angle), the set is applicable to other daylight times (or solar  
97 zenith angles). Thus this simple expression provides a  
98 reasonably accurate estimate of fractional sky cover. It is  
99 worth emphasizing that for a good estimation the wave-  
100 length pair for the transmittance ratio should be separated  
101 enough to have a substantial contrast of aerosol optical  
102 depth between the two wavelengths. Moreover, at both  
103 wavelengths the potential interference of gaseous absorp-  
104 tion, particularly water vapor due to cloud-water vapor  
105 interaction, should be minimal.

106 [7] To illustrate the underlying principles and sensitivity,  
107 a pair of multifilter rotating shadowband radiometer  
108 (MFRSR) channels at 415 and 860 nm, where gaseous  
109 absorption is minimal, is selected for forward simulation.  
110 The MFRSR is a seven-channel radiometer with six pass-  
111 bands 10 nm Full Width Half Maximum (FWHM) centered  
112 near 415, 500, 610, 665, 860, and 940 nm, and an unfiltered  
113 silicon pyranometer [Harrison et al., 1994]. It uses an  
114 automated shadowbanding technique to measure the total-  
115 horizontal, diffuse-horizontal, and direct-normal spectral

irradiances through a single optical path. The diffuse- 116  
horizontal irradiance represents downwelling hemispheric 117  
irradiance with an effective  $160^\circ$  field of view. The Langley 118  
regression of the direct-normal irradiance taken on clear 119  
stable days can be used to extrapolate the instrument's 120  
response to the top of the atmosphere, and this calibration 121  
can then be applied to all components of irradiance. Trans- 122  
mittances can be subsequently calculated under cloudy 123  
conditions as the ratio of the uncalibrated output to the 124  
extrapolated top-of-the-atmosphere value. The diffuse 125  
transmittance is a normalized diffuse radiation by the 126  
corresponding solar constant inferred from Langley regres- 127  
sion. Therefore the transmittance ratio at two wavelengths is 128  
independent of absolute calibration. Accurate measurements 129  
of atmospheric transmittance from a MFRSR will ensure the 130  
accuracy of retrieval of aerosol optical depth during the 131  
clear-sky periods and cloud optical depth under cloud 132  
conditions [Harrison et al., 1994; Min and Harrison, 133  
1996; Min et al., 2004; Wang and Min, 2008]. 134

[8] Using a radiative transfer model [Min et al., 2004], 135  
transmittance ratios at the two chosen nongaseous absorp- 136  
tion wavelengths are simulated under various cloudy and 137  
clear-sky conditions for different solar zenith angles. In the 138  
simulation, surface albedos of 0.036 and 0.25 are used for 139  
415 and 860 nm, respectively, representing normal vegetat- 140  
ed surface. Under clear-sky conditions with climatologic 141  
background aerosols (Angstrom exponents of 1.12 and 142  
1.58, and optical depth up to 0.35), as shown in Figure 2a, 143  
the transmittance ratio varies from 0.10 to 0.35. Changes of 144  
aerosol size and optical depth as well as solar zenith angle 145  
within the normal ranges would result in an uncertainty of 146  
about 0.1 around the clear-sky baseline of transmittance ratio. 147  
In reality, the clear-sky baseline, as well as aerosol prop- 148  
erty, can be accurately determined from the measurements 149  
during the clear-sky periods. Thus uncertainty of the clear- 150  
sky baseline should be substantially smaller. 151

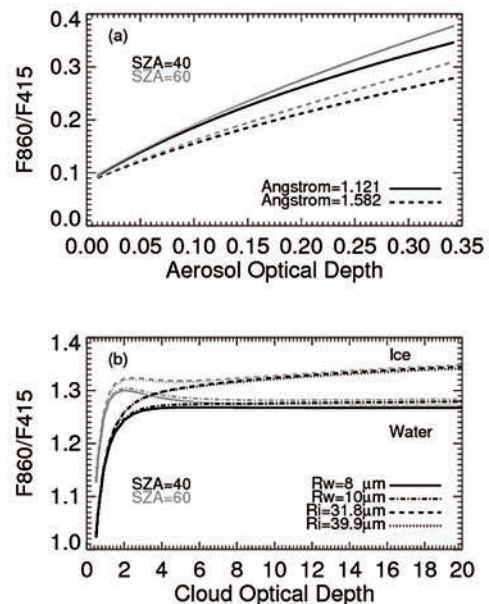


**Figure 2.** Simulated spectral ratios for various aerosol (a) and cloud (b) conditions.



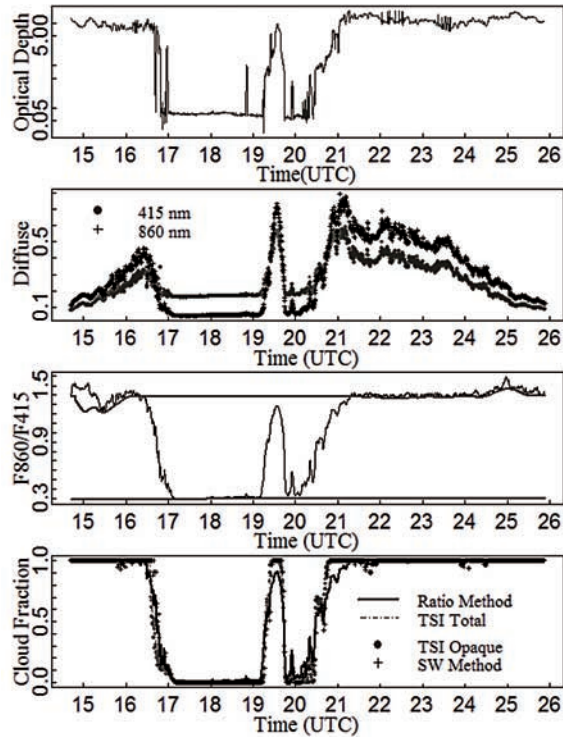


**Figure 3.** Retrieved aerosol and cloud optical depths (logarithmic scale), measured diffuse irradiances for 415 and 860 nm, spectral ratio and associated cloudy (the upper line) and clear-sky (the lower line) baselines, and retrieved and observed cloud fractions on 10 July 2005 at Pt. Reyes.

[9] As shown in Figure 2b, the transmittance ratio for both ice and water clouds varies from 1 to the asymptote values of 1.25 and 1.34 for water and ice clouds, respectively. The surface albedo,  $a$ , impact on diffuse irradiance can be simply parameterized as  $F/(1 - a)$ , where  $F$  is diffuse irradiance with the dark surface ( $a = 0$ ). The transmittance ratio with assumed albedos of 0.036 and 0.25 for 415 and 860 nm, respectively, can be expressed as

$$\begin{aligned} \left( \frac{F_{860}}{1 - a_{860}} \right) / \left( \frac{F_{415}}{1 - a_{415}} \right) &= \frac{F_{860}}{F_{415}} (1 - a_{415}) / (1 - a_{860}) \\ &= 1.28 * \frac{F_{860}}{F_{415}} \end{aligned}$$

[10] Because of  $\frac{F_{860}}{F_{415}} \approx 1$  under cloudy conditions, the transmittance ratios are greater than 1 as a result of a higher surface albedo at 860 nm.

[11] It is clear that the asymptote value, reached at modest cloud optical depth of 6, is insensitive to the solar zenith angles. The difference of transmittance ratio because of a 20-degree change of solar zenith angle is about 0.01 when the cloud optical depth is greater than 6. The maximum difference of transmittance ratio because of a 20-degree change of solar zenith angle, occurred at cloud (or aerosol) optical depths between 0.35 and 3, is about 0.1. Furthermore, different effective sizes of cloud particles within the same cloud thermodynamic phase have negligible effect on

the transmittance ratio. Again, the cloudy baseline of transmittance ratio can be directly determined during periods with large cloud optical depths from the time series of the measurements. Changes of cloud property (effective radius and optical depth) during broken periods will have very small effect on the localized cloudy baseline. Overall uncertainty associated with cloud, aerosol, and solar zenith angle variations using a climatologic baseline set are about 0.2, 20% of the dynamic range of transmittance ratio. Therefore the maximum uncertainty for the fractional sky cover is 20%. As pointed out previously, in reality, both clear-sky and cloudy baselines can be directly determined from the time series of measurements, and thus the uncertainty of cloud fraction retrieval should be substantially reduced. Given possible changes of cloud, aerosol, and solar zenith angle during the broken cloud periods, as estimated from real measurements, the uncertainty is estimated at about 10%.

### 3. Validation

[12] Validation and evaluation of retrieved products are key to showing the effectiveness of a retrieval algorithm. We processed the MFRSR measurements taken during the Marine Stratus Radiation Aerosol and Drizzle (MASRAD) field campaign at Point Reyes, California in 2005, where a Total Sky Imager (TSI) with a hemispherical field of view (FOV) was deployed and provided time series of fractional sky cover. Also the estimation of fractional sky cover from measured surface broadband SW radiation was available during the field campaign for intercomparison [Long *et al.*, 2006a]. The TSI cloud classifications are dependent on pixel color, as are clear-sky and clouds themselves depending on their optical depth. Roughly, distinctly blue pixels are labeled as clear-sky, where white/gray/dark gray colors produced by optically thick clouds are labeled as opaque cloud [Long *et al.*, 2006b]. The SW method was developed using sky imager retrievals that were carefully manually screened for consistent classification results as a training reference [Long *et al.*, 2006a]. The SW retrieval methodology uses the effect of clouds on the diffuse downwelling (measured minus clear-sky diffuse SW), normalized by the corresponding clear-sky downwelling total SW to remove the solar zenith angle dependence. Thus rather than a pixel-by-pixel determination of cloud/no cloud associated with sky imager retrievals, the aggregate hemispheric effect on the downwelling SW irradiance is used to estimate sky cover. Thus the SW method is far more similar to the MFRSR method described here than are sky imager retrievals.

[13] 10 July 2005 was a partly cloudy day, with overcast conditions occurring in both early morning and afternoon and several hours of clear-sky periods in between. The sum of aerosol optical depth and cloud optical depth, retrieved from direct and global radiation measurements [Min and Harrison, 1996; Min *et al.*, 2004; Wang and Min, 2008], shown in Figure 3a, varied from 18.5 to 0.05. The diffuse radiation at 860 nm, shown in Figure 3b, changed from greater than to less than the diffuse radiation at 415 nm, corresponding to the atmospheric optical depth variation. Although the diffuse radiation at both 415 and 860 nm varied systematically with solar zenith angle (Figure 3b), the ratio between the two was fairly constant at a value of 1.38

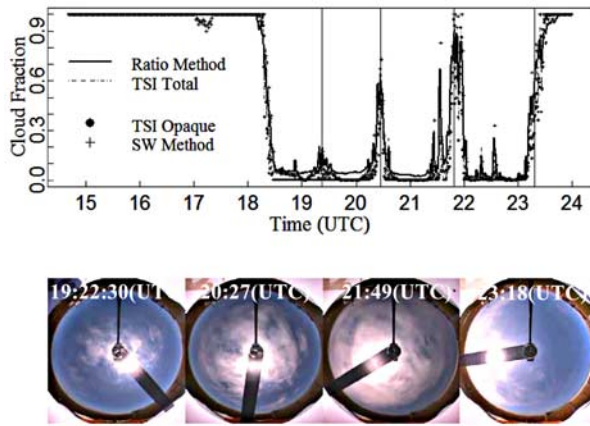


**Figure 4.** Retrieved and observed cloud fractions and corresponding TSI cloud imagers on 8 July 2005 at Pt Reyes.

235 when cloud optical depths were greater than 6 (Figure 3c).  
 236 This result verifies our assertion in the sensitivity study that  
 237 transmittance ratio approaches an asymptote value for thick  
 238 clouds and such a value is insensitive to the solar zenith angle  
 239 as the solar zenith angle varied from 17 to 75 degrees.  
 240 Therefore the cloudy baseline is defined as the minimum  
 241 value during overcast thick cloud periods.

242 [14] Clouds generally change much more rapidly than  
 243 clear-sky aerosols, allowing one to distinguish clear-sky  
 244 periods based on temporal variation of atmospheric optical  
 245 depth derived from direct beam measurements. In practice  
 246 we define a clear-sky period as the standard deviation of  
 247 optical depths inferred from direct beam radiation during  
 248 the period is less than 0.01, which implies that the  
 249 detection threshold of minimal cloud optical depth is  
 250 0.01. The retrieved aerosol optical depths between 17:20  
 251 to 19:00 UTC were about 0.06 with very small variation  
 252 (less than 0.006), combined with the low values and small  
 253 variation of diffuse transmittance, indicating it was a clear-  
 254 sky period. The mean transmittance ratio of 0.30 during the  
 255 period therefore is defined as the clear-sky baseline. Thus,  
 256 for a typical broken cloudy day, both clear-sky and cloudy  
 257 baselines are determined directly from the time series of  
 258 measurements. As surface albedos will not change dramati-  
 259 cally in days, if a day has no long-term (~one hour) clear-  
 260 sky or overcast cloudy periods to define the baseline, the  
 261 baselines defined before or after that day will provide good  
 262 estimates for the day. Furthermore, such a localized baseline  
 263 procedure of the transmittance ratio does not require a good  
 264 absolute calibration of the radiometer as long as the instru-  
 265 ment is stable and has a good reproducibility at the two  
 266 wavelength channels. Therefore the ratio method with the  
 267 localized baseline procedure will tend to reduce the uncer-  
 268 tainty of the sky cover retrievals.

269 [15] With defined baselines, the fractional sky cover is  
 270 readily retrieved using equation 3. Figure 3d shows compar-  
 271 ison among three different instruments and four different  
 272 results of fractional sky cover. The TSI reports both thick  
 273 opaque cloud cover and total cloud cover that includes thin  
 274 clouds. In this case, the total and opaque cloud covers are  
 275 the same from TSI, indicating the clouds present were  
 276 opaque. It is clear that retrievals of the ratio method agree  
 277 well with the other three results.

[16] 8 July 2005 is another broken cloudy day with 278  
 several clear-sky periods, shown in Figure 4. Various cloud 279  
 distributions in the sky, illustrated by TSI images at four 280  
 particular times, are well monitored by the ratio method. 281  
 Overall agreement of retrieved cloud fraction is very good 282  
 with both TSI measurements and SW method, absolute 283  
 differences of 0.030 and 0.028, respectively. 284

[17] However, there are some occasions that differences 285  
 among these methods are substantial, for example on 286  
 16 March 2005, shown in Figure 5. For the cloudy condi- 287  
 tion illustrated by the TSI image at 16:24 UTC, the TSI total 288  
 cloud cover is larger than the TSI opaque cloud cover, 289  
 indicating some thin clouds present at the time. Both the 290  
 ratio and SW methods agree with the TSI total cloud cover. 291  
 However, at 17:24 and 19:30 UTC, shown in TSI images, 292  
 sky cover retrieved by the ratio method agrees better with 293  
 the TSI opaque sky cover and is substantially lower than the 294  
 TSI total cloud cover. The SW retrievals tend to agree with 295  
 results of the ratio method. The classification as thin cloud 296  
 (optically thinner cloud that is blue-tinted because the clear- 297  
 sky background can be seen through them) for a TSI is less 298  
 robust, in part due to the proprietary auto white balance 299  
 function of the commercial camera used in the TSI which 300  
 adjusts the overall image color rendering dependent on how 301  
 much of the image contains white pixels. In effect, less 302  
 opaque cloudiness in the image produces slightly more 303  
 sensitivity to optically thin clouds in the retrievals. Addi- 304  
 tionally, each camera differs slightly in image color render- 305  
 ing characteristics, yet the baseline clear-sky library 306  
 included in the processing software was generated using 307  
 one particular camera at YES headquarters in Connecticut, 308  
 USA. Thus individual camera behavior and characteristics 309  
 effectively make the clear/thin threshold less robust than the 310  
 classification of obviously clear skies and opaque clouds. In 311  
 this case, the threshold of thin clouds for the TSI algorithms 312  
 may be too low, resulting in an overestimation of the total 313  
 sky cover. There is a period around 20:00 UTC, however, 314  
 where the four retrievals differ significantly. The differences 315  
 may be due in part to previously discussed threshold issues 316  
 of thin and opaque clouds and different effective fields of 317  
 view of the three instruments. The retrievals of the ratio 318

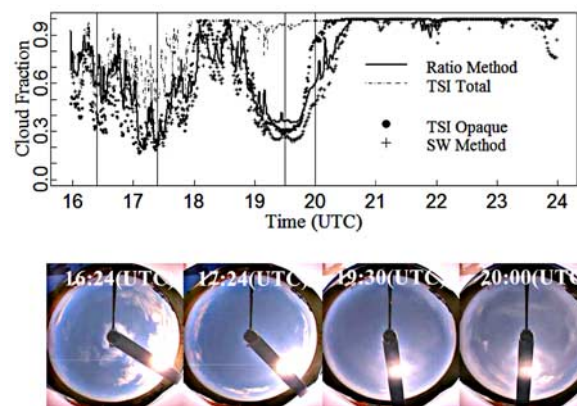


**Figure 5.** Retrieved and observed cloud fractions and corresponding TSI cloud imagers on 16 March 2005 at Pt Reyes.



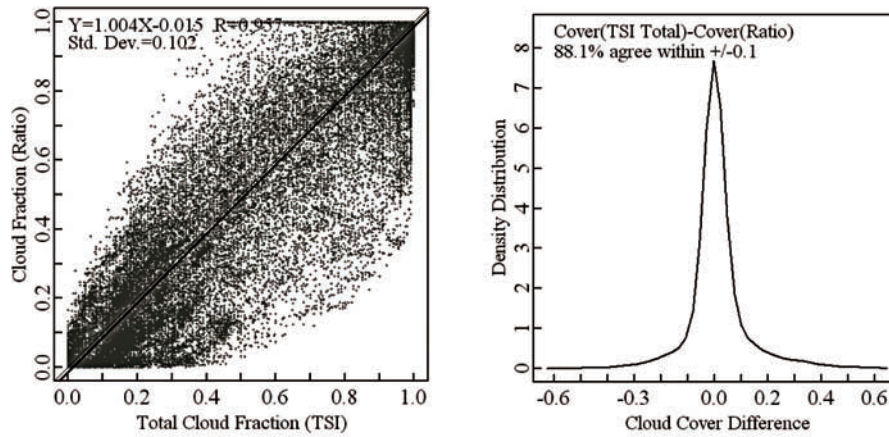


**Figure 6.** Scatterplot of TSI measurements and retrieved cloud fraction from spectral ratio method, and cloud fraction difference distribution for the entire field campaign.

319 method lie in between the TSI and SW values, and are  
320 closer to the SW retrievals.

321 [18] While the case studies provide insight on the perfor-  
322 mance of this new retrieval algorithm, a more extensive  
323 evaluation is required. Statistical evaluation has been con-  
324 ducted using measurements over the entire MASRAD field  
325 campaign from March to September 2005. Since different  
326 instruments have different sampling rates, synchronization  
327 of measurements and data quality control have been applied  
328 to produce a 1-minute sky cover data set with 85498  
329 samples from all three instruments. Figure 6 shows the  
330 comparison between TSI total sky cover and the ratio-  
331 method retrievals. The slope of regression is 1.004 with  
332 an intercept of 0.015, indicating our assumption of linear  
333 partition between cloud transmittance ratio and clear-sky  
334 transmittance ratio is practical. The correlation coefficient is  
335 0.957 with a standard deviation of 0.102 and a mean bias of  
336 0.02. These statistics indicate good agreement between the  
337 two methods. As shown in Figure 6b, over 88.1% of data  
338 samples agree within 0.1. The residual differences may  
339 be due to (1) different sensitivities to very thin clouds;  
340 (2) different FOVs; and (3) the calibration issue of TSI.

[19] The statistics between the ratio and SW methods, 341  
shown in Figure 7, have a better correlation coefficient 342  
(0.975) and smaller standard deviation (0.075) with a 343  
slightly smaller slope (0.961) than that between TSI and 344  
ratio methods. Over 92.5% of the samples have a difference 345  
smaller than 0.1. The better agreement between the ratio and 346  
SW methods is not surprising, given that both methods are 347  
based on radiometry measurements. Nonetheless these 348  
longer-term comparisons demonstrate that the simple ratio 349  
method provides a good estimate of fractional sky cover 350  
under various conditions. 351

#### 4. Discussion and Conclusion 352

[20] Clouds remain the greatest sources of uncertainty in 353  
global climate change research. Changes in cloud amount 354  
through climate feedback may well be one of the signs of 355  
climate change. It is crucial to accurately monitor fractional 356  
sky cover with high spatial and temporal resolution globally. 357  
In this study, a ratio method for estimating fractional sky 358  
cover from spectral radiation measurements has been 359  
proposed. It is based on spectral characteristics of clouds 360  
and clear-sky aerosols to partition sky fraction. As illustrated 361

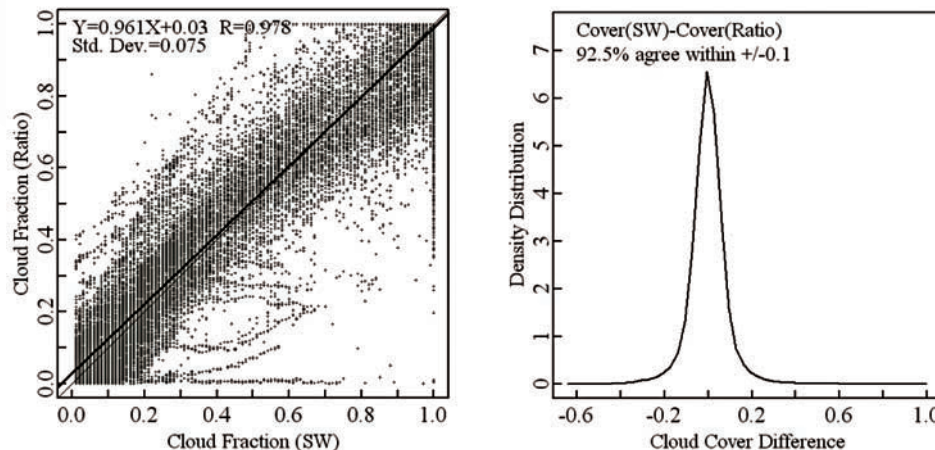


**Figure 7.** Scatterplot of retrieved cloud fraction from spectral ratio method and SW method, and cloud fraction difference distribution for the entire field campaign.

362 in our sensitivity study and demonstrated in real measure-  
 363 ment comparisons, the transmittance ratio at selected wave-  
 364 lengths is insensitive to solar zenith angle and major  
 365 atmospheric gaseous absorption. With a localized baseline  
 366 procedure, retrievals of this ratio method are independent of  
 367 absolute calibration and weakly sensitive to changes of  
 368 cloud and aerosol optical properties, and thus substantially  
 369 reduce the retrieval uncertainty. The uncertainty of this ratio  
 370 method once localized, estimated through sensitivity study  
 371 and intercomparison, is less than 10%.

372 [21] Narrowband spectral measurements are now widely  
 373 available, for example, hundreds of MFRSRs have been  
 374 deployed globally. This simple ratio method will substan-  
 375 tially enhance current capability of monitoring fractional  
 376 sky cover in large geographic distribution, providing a great  
 377 opportunity to monitor climate change in terms of cloud  
 378 amount.

379 [22] **Acknowledgments.** This research was supported by the Office  
 380 of Science (BER), U.S. Department of Energy, Grant DE-FG02-  
 381 03ER63531, and by the NOAA Educational Partnership Program with  
 382 Minority Serving Institutions (EPP/MSI) under cooperative agreements  
 383 NA17AE1625 and NA17AE1623. Surface data were obtained from the  
 384 Atmospheric Radiation Measurement (ARM) Program sponsored by the  
 385 U.S. Department of Energy, Office of Energy Research, Office of Health  
 386 and Environmental Research, Environmental Sciences Division.

## 387 References

- 388 Angstrom, A. (1929), On the transmission of sun radiation and on dust in  
 389 the air, *Geogr. Ann.*, 2, 156–166.
- 390 Clothiaux, E., et al. (1999), The atmospheric radiation measurement pro-  
 391 gram cloud radars: Operational modes, *J. Atmos. Sci.*, 56, 819–827.
- 392 Fairall, C., and J. Hare (1990), An eight-month sample of marine stratocu-  
 393 mulus cloud fraction, albedo and integrated liquid water, *J. Clim.*, 3,  
 394 847–864.
- Harrison, L. C., J. J. Michalsky, and J. Berndt (1994), Automated multifilter  
 395 rotating shadowband radiometer: An instrument for optical depth and  
 396 radiation measurements, *Appl. Opt.*, 33(22), 5118–5125. 397
- IPCC (2007), *Climate Change*. 398
- Long, C. N., and T. P. Ackerman (2000), Identification of clear skies from  
 399 broadband pyranometer measurements and calculation of downwelling  
 400 shortwave cloud effects, *J. Geophys. Res.*, 105(D12), 15,609–15,626. 401
- Long, C. N., T. P. Ackerman, K. L. Gaustad, and J. N. S. Cole (2006a),  
 402 Estimation of fractional sky cover from broadband shortwave radio-  
 403 meter measurements, *J. Geophys. Res.*, 111, D11204, doi:10.1029/  
 404 2005JD006475. 405
- Long, C. N., J. M. Sабburg, J. Calbo, and D. Pages (2006b), Retrieving  
 406 cloud characteristics from ground-based daytime color all-sky images,  
 407 *J. Tech.*, 23(5), 633–652. 408
- Min, Q. L., and L. C. Harrison (1996), Cloud properties derived from  
 409 surface MFRSR measurements and comparison with GOES results at  
 410 the ARM SGP site, *Geophys. Res. Lett.*, 23(13), 1641–1644. 411
- Min, Q., E. Joseph, and M. Duan (2004), Retrievals of thin cloud optical  
 412 depth from a multifilter rotating shadowband radiometer, *J. Geophys.*  
 413 *Res.*, 109, D02201, doi:10.1029/2003JD003964. 414
- Minnis, P. (1989), Viewing zenith angle dependence of cloudiness deter-  
 415 mined from coincident GOES EAST and GOES WEST data, *J. Geophys.*  
 416 *Res.*, 94(D2), 2303–2320. 417
- Pfister, G., R. L. McKenzie, J. B. Liley, A. Thomas, B. W. Forgan, and  
 418 C. N. Long (2003), Cloud coverage based on all-sky imaging and its  
 419 impact on surface solar irradiance, *J. Appl. Meteorol.*, 42(10), 1421–  
 420 1434. 421
- Randall, D., J. Coakley Jr., C. Fairall, R. Kropfli, and D. Lenschow (1984),  
 422 Outlook for research on subtropical marine stratiform clouds, *Bull. Am.*  
 423 *Meteorol. Soc.*, 65, 1290–1301. 424
- Rossow, W., A. Walker, and L. Garder (1993), Comparison of ISCCP and  
 425 other cloud amounts, *J. Clim.*, 6, 2394–2418. 426
- Wang, T., and Q. Min (2008), Retrieving optical depths of optically thin and  
 427 mixed-phase clouds from MFRSR measurements, *J. Geophys. Res.*,  
 428 doi:10.1029/2008JD009958, in press. 429
- M. Duan, Institute of Atmospheric Physics, Chinese Academy of  
 430 Science, Beijing, China. 432
- C. N. Long, Pacific Northwest National Laboratory, Richland, WA, USA. 433
- Q. Min and T. Wang, Atmospheric Sciences Research Center, State  
 434 University of New York, Room L215, 251 Fuller Road, Albany, NY 12203,  
 435 USA. (min@asrc.cestm.albany.edu) 436

American Geophysical Union  
Author Query Form

Journal: **Journal of Geophysical Research - Atmospheres**  
Article Name: Min (**2008JD010278**)

---

Please answer all author queries.

1. Please provide division/department of affiliation 3.
2. Please provide complete mailing address (building/street address/department/division/PO Box/postal code) of authors M. Duan and C.N. Long.
3. Please provide complete reference information of reference "*IPCC, 2007*".
4. Please check if journal title of reference "*Long et al., 2006b*" was captured correctly.